arXiv:1303.6648v1 [astro-ph.CO] 26 Mar 2013

The Embedded Transparent Lens and Fermat's Least-Time Principle

R. Kantowski,[1,*] B. Chen,[1,†] and X. Dai[1,‡]

[1]*Homer L. Dodge Department of Physics and Astronomy,*
University of Oklahoma, 440 West Brooks, Norman, OK 73019, USA

(Dated: March 28, 2013)

Abstract

We present a much simplified version of the embedded point mass lens theory and then make the obvious extension of this theory to any embedded transparent lens. Embedding a lens effectively reduces the gravitational potential's range, i.e., partially shields the lensing potential because the lens mass is made a contributor to the mean mass density of the universe and not simply superimposed upon it. This presentation results from simplifying previous formulations of the embedded point mass theory and is quite similar to the standard theory. We are then able to re-derive the simplified point mass theory by applying Fermat's least-time principle to the time-delay function. Even though rigorous derivations are only made for the point mass, the lens equation to the lowest order for any distributed lens, is obvious. We find from this simplified theory that embedding can introduce corrections at the few percent level in weak lensing shears caused by large clusters but only at large impacts. The potential part of the time delay is also affected in strong lensing at the few percent level. Additionally we are surprised to find that the cosmological constant is only present in this theory at a higher order.

PACS numbers: 98.62.Sb

Keywords: General Relativity; Cosmology; Gravitational Lensing;

In this Letter we present a simplified version of the embedded point mass lens theory [1–4] that can easily be used by anyone familiar with conventional lensing theory, see Eqs. (5)-(10). Because we have succeeded in replacing image impact position variables by the image's angular position θ_I (Fig. 1), we have succeeded in giving the point mass lens equation in a form which is easily compared with the conventional theory [see Eq. (13)]. Image properties such as the time delay, i.e., the excess time light takes to reach the observer because it encounters the embedded lens, are also given. By applying Fermat's least time principle [5, 6] to this time-delay function the lens equation to lowest order is then consistently arrived at [see Eq. (5)], i.e., it is the same as the lowest order term in the rigorously derived result, Eq. (13). Because we can interpret this lowest order equation within the conventional theory as lensing by a point mass plus a negative surface mass density [see Eqs. (9) and (14)], we are able to extend this theory to any embedded transparent lens, see Eqs. (15) and (16).

---

[*] kantowski@ou.edu

[†] bchen@ou.edu

[‡] xdai@ou.edu

In previous work [1–4] we have investigated, in depth, effects of embedding on the point mass lens equation and on all resulting image properties. However, application of that theory is quite complex because of the lens impact variables used. Our embedded lens model remains a spherical comoving mass void (see Fig. 1) in a flat pressureless Friedman-Lemaître-Robertson-Walker (FLRW) universe, containing the cosmic mass m removed from the void condensed at its center [7, 8]. The actual geometry in the void is described by the Kottler metric [9] which is similar to Schwarzschild's geometry but with the addition of a cosmological constant Λ. This lens model is used to maintain absolute correctness of the gravity theory and hence avoid approximation errors in the lensing theory. A universe filled with such voids is called a Swiss cheese universe and has historically been used to compute effects of inhomogeneities on distance-redshift relations [10–15] and on the anisotropy of the CMB [16]. The comoving radius χ_b of a lens void at redshift z_d is related to the Schwarzschild radius $r_s \equiv 2G\mathrm{m}/c^2$ of the embedded lens by

$$r_s = \Omega_\mathrm{m} \frac{H_0^2}{\mathrm{c}^2} \chi_b^3, \tag{1}$$

where H_0 is the Hubble constant, Ω_m is the usual matter density parameter, and the current radius of the flat universe has been taken equal to 1. The lens void expands with the background cosmology and had a physical radius $r_d = \chi_b/(1+z_d)$ when the observed photons passed the deflector. Throughout a subscript 'd' on evolving quantities means evaluated at the deflector's redshift z_d. We start by presenting the new point mass results, explain how they were arrived at from the previous more complicated expressions, and then explain how they are generalized to distributed lenses.

Only two parameters appear in the simplified point mass theory, the familiar angular Einstein ring radius

$$\theta_E \equiv \sqrt{\frac{2\ r_s D_{ds}}{D_d D_s}}, \tag{2}$$

and the maximum value of the angular image position θ_I (see Fig. 1)

$$\theta_M \equiv \frac{r_d}{D_d} = \frac{\chi_b}{\chi_d}. \tag{3}$$

where χ_d is the FLRW comoving distance to the deflector from the observer and D_d, D_s, and D_{ds} are angular diameter distances, respectively of the deflector, source, and source relative to the deflector. The maximum image angle θ_M occurs for the primary image when the light ray from the source just grazes the spherical void and can be thought of as the

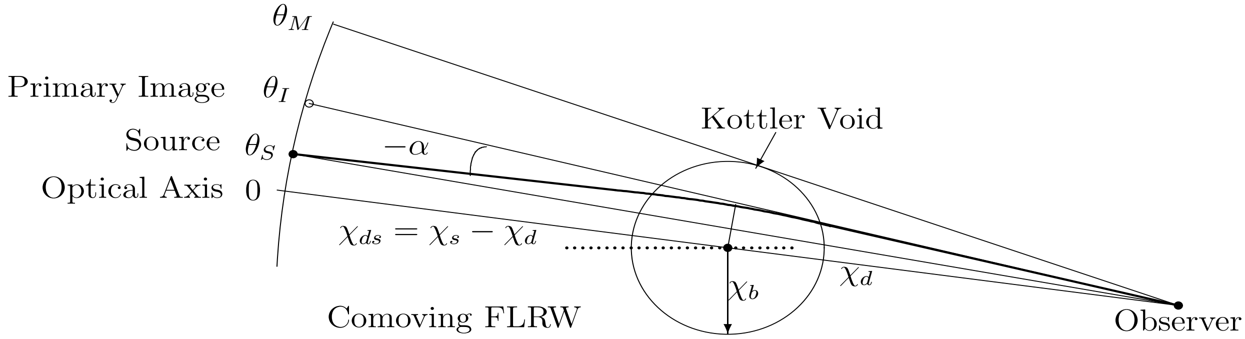

FIG. 1. A photon travels from a source located at angular position θ_S, a comoving distance χ_s from the observer, and enters a Kottler void of comoving radius χ_b centered at comoving distance χ_d from the observer. The photon is deflected by an angle α (< 0) and returns to the FLRW dust on its way to the observer, where it appears at angle θ_I. The maximum image angle θ_I is θ_M and occurs when the light ray grazes the Kottler void.

angular size of the embedded void as seen by the observer. For this maximum image angle, the deflection angle is zero and the source is likewise located at θ_M. For a massive galaxy or a cluster lens ($M = 10^{12} M_\odot$ or $10^{15} M_\odot$) at redshift $z_d = 0.5$, and a source at $z_s = 1.0$, the Einstein ring radius θ_E is respectively $1''.66$ or $52''.6$, much smaller than the maximum image angle, i.e., $\theta_E/\theta_M = 0.0085$ or 0.027. Consequently both strong and weak lensing effects are seen within the void. By using θ_I as the independent image variable we find from our previous work [1–4] that up to a constant, the time-delay function cT (accurate to order $\boldsymbol{\delta}^1$, explained below) is

$$cT(\theta_S, \theta_I) = (1+z_d)\frac{D_d D_s}{D_{ds}}\left\{\frac{(\theta_S-\theta_I)^2}{2} - \theta_E^2\left[\frac{1}{2}\log\left(\frac{\theta_I/\theta_M}{1+\sqrt{1-(\theta_I/\theta_M)^2}}\right)^2 \right.\right.$$
$$\left.\left. + \frac{1}{3}\left[4-(\theta_I/\theta_M)^2\right]\sqrt{1-(\theta_I/\theta_M)^2} + \mathcal{O}\big(\boldsymbol{\delta}^2\big)\right]\right\}. \tag{4}$$

This expression, without the $(1+z_d)$ factor, is often called the *Fermat potential*, see [17]. It represents the difference in arrival times of two signals originating at a source at redshift z_s, one traveling on a straight path entirely in FLRW and the other encountering the embedded deflector at redshift z_d (see Fig. 1). It is the sum of a geometric and a potential term [2, 18] written in a form to which Fermat's principle can be applied [5, 6]. By varying $cT(\theta_S, \theta_I)$ with respect to the image angle θ_I, i.e., by applying Fermat's least time principle, we obtain the embedded lens equation, accurate to order $\boldsymbol{\delta}^1$,

$$\theta_S = \theta_I - \frac{\theta_E^2}{\theta_I}\left[\sqrt{1-(\theta_I/\theta_M)^2}\right]^3. \tag{5}$$

The conventional linear lensing result, without embedding, is regained by neglecting the (θ_I/θ_M) term.

From Eq. (5) the inverse image matrix eigenvalues (respectively axial and radial) are found to be

$$a_\phi = \frac{\theta_S}{\theta_I} = 1 - \left(\frac{\theta_E}{\theta_I}\right)^2\left[\sqrt{1-(\theta_I/\theta_M)^2}\right]^3, \tag{6}$$

$$a_r = \frac{d\theta_S}{d\theta_I} = 1 + \left(\frac{\theta_E}{\theta_I}\right)^2\left[1+2\,(\theta_I/\theta_M)^2\right]\sqrt{1-(\theta_I/\theta_M)^2}. \tag{7}$$

The reciprocal amplification is

$$\mu^{-1} = a_\phi a_r = 1 + 3\left(\frac{\theta_E}{\theta_M}\right)^2\sqrt{1-(\theta_I/\theta_M)^2} - \left(\frac{\theta_E}{\theta_I}\right)^4\left[1+2\,(\theta_I/\theta_M)^2\right]\left[1-(\theta_I/\theta_M)^2\right]^2, \tag{8}$$

with a normalized effective surface mass density κ present

$$\kappa = 1 - (a_\phi + a_r)/2 = -\frac{3}{2}\left(\frac{\theta_E}{\theta_M}\right)^2\sqrt{1-(\theta_I/\theta_M)^2}. \tag{9}$$

This negative term can be interpreted as the void mass removed from the observing light beam at image position θ_I. The shear in the bundle of light rays at image position θ_I is

$$\gamma = (a_r - a_\phi)/2 = \frac{1}{2}\left(\frac{\theta_E}{\theta_I}\right)^2\left[2+(\theta_I/\theta_M)^2\right]\sqrt{1-(\theta_I/\theta_M)^2}. \tag{10}$$

By neglecting the θ_E/θ_M and θ_I/θ_M terms, i.e., the shielding terms caused by embedding, the above expressions all reduce to the conventional non-embedded values. These results represent a significant simplification in our previous work on embedded lenses and can easily be used without following the complexities of their derivation outlined next. The generalization of the above point mass lens equation, Eq. (5), to spherically distributed and arbitrarily distributed lenses is given respectively in Eqs. (15) and (16). In Fig. 2 on the left we have plotted the shear γ as a function of θ_I and have compared the embedded γ with the conventional value for a large cluster lens. The shear is seen to differ from the conventional Schwarzschild value by more than a few percent but only at impact angles more than $15\,\theta_E$. In Fig. 2 on the right we have plotted time delay differences caused by embedding. These differences are primarily due to the potential part of Eq. (4) differing from the Schwarzschild value at large primary image angles.

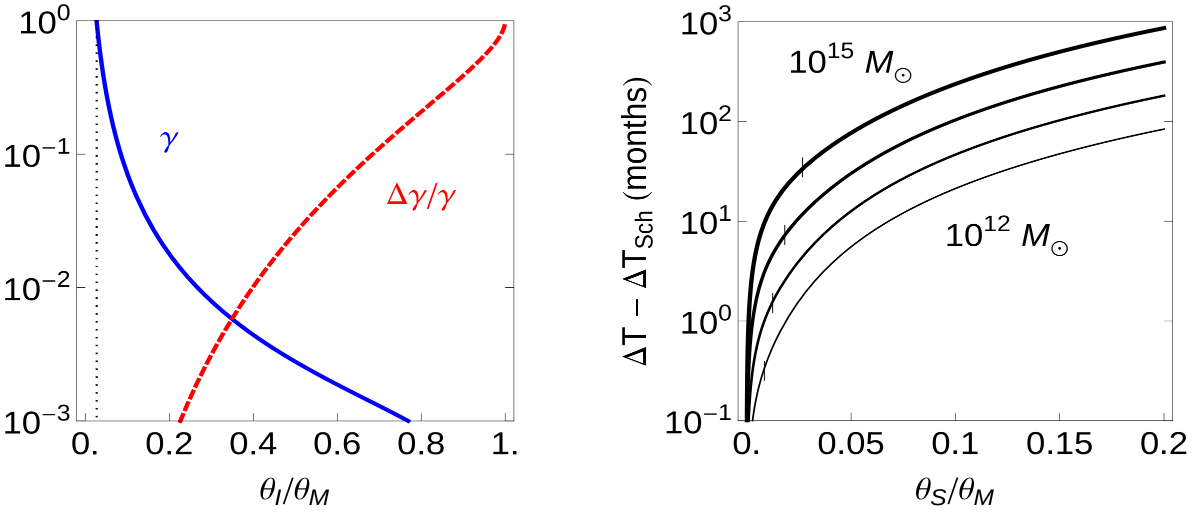

FIG. 2. (Left) Embedding corrections to the image shear γ for a $10^{15} M_\odot$ cluster lens. The source and lens redshifts are $z_s = 1.0$ and $z_d = 0.5$, respectively. The solid blue curve is the shear, γ, and the dashed red curve is the fractional difference in the image shear, $\Delta\gamma/\gamma$, caused by embedding. Both are plotted as a functions of θ_I/θ_M where the Einstein ring radius is $\theta_E = 52''\!.6$, the void radius is $\theta_M = 32'\!.8$, and $\theta_E/\theta_M = 0.027$ is the vertical dotted line. (Right) The difference in the embedded time delay and the conventional Schwarzschild time delay, $\Delta T - \Delta T_{\mathrm{Sch}}$, computed using Eq. (4) and the Schwarzschild equivalent for the primary and secondary images, is plotted as a function of source position angle θ_S/θ_M. The time delay difference is given in months for four point mass lenses, $m = 10^{15} M_\odot, 10^{14} M_\odot, 10^{13} M_\odot$, and $10^{12} M_\odot$ (respectively top to bottom curves). The small vertical ticks on each curve are at respective θ_E/θ_M values.

The rigorously derived embedded point mass lens equation, Eq. (13), and from it the lowest order term Eq. (5), follows from our earlier work [1, 2] where we computed the lens equation and other lensing quantities as functions of two impact variables of the Kottler metric, the minimum impact radius r_0 and the void impact angle $\tilde{\phi}_1$ (see Fig. 1 of [4]). In [3, 4] we succeeded in eliminating the minimum impact radius r_0 in favor of the single void impact angle $\tilde{\phi}_1$ and were consequently able to write the lens equation, etc., as functions of $\tilde{\phi}_1$ alone. Only now have we succeeded in eliminating $\tilde{\phi}_1$ in favor of observable θ_I and truly simplifying the point mass embedded lens equation as given in Eq. (13).

The conventional linear lensing theory is only an approximate theory for a variety of reasons including the fact that its two fundamental ingredients, the bending angle $\alpha =$

$-2r_s/r_0$, and the image position $\theta_I = r_0/D_d$, are both lowest order approximations, see [1, 2]. Obvious corrections to α require terms of order $(r_s/r_0)^2$ and geometry corrections are required for θ_I. In addition to these obvious corrections we have investigated corrections that come from insisting that the gravity theory confirm to Einstein's. Such insistence requires the deflector contribute to the mean cosmological mass density, i.e., that it is embedded in the background cosmology. To track all corrections we have ordered them by their magnitudes using a parameter $\boldsymbol{\delta}$, whose value is 1. In [1–4] the details of tracing a ray from a source at redshift z_s through its interaction with an expanding void at redshift z_d was done using a series of approximation of orders up to $\boldsymbol{\delta}^4$ to obtain the needed accuracy, e.g., to evaluate the time delay as given in Eq. (4), see Eqs. (10) and (14) of [2] and Eqs. (22) and (23) of [4]. When observing galaxies and clusters at cosmological distances, lensing parameters of order $\boldsymbol{\delta}^1$ are the angular void radius θ_M, see Eq. (3), and β_d, the expansion rate of the void's boundary as measured by static observers in the void

$$\beta_d \equiv \frac{v_d}{c} = \sqrt{r_s/r_d + \Lambda r_d^2/3} = \frac{H_d}{c} r_d, \tag{11}$$

where H_d is the Hubble parameter at the lens redshift z_d. Equation (11), as well as Eq. (1), are consequences of the geometry of embedding. When r_s/r_d and $\Lambda r_d^2/3$ appear individually they were both treated as terms of order $\boldsymbol{\delta}^2$. For the galaxy and cluster lens discussed above, $\boldsymbol{\delta}^1$ terms are of respective orders $\lesssim 10^{-3}$ and $\lesssim 10^{-2}$.

The steps we followed to obtain the simplified embedded theory were as follows: By inverting Eq. (8) of [4] we obtained the previously used impact variable $\tilde{\phi}_1$ as a function of θ_I,

$$\tilde{\phi}_1 = \sin^{-1}(\theta_I/\theta_M) + \boldsymbol{\delta}\beta_d\,(\theta_I/\theta_M) - \boldsymbol{\delta}^2 \left\{ \frac{\theta_M^2}{6} \frac{(\theta_I/\theta_M)^3}{\sqrt{1-(\theta_I/\theta_M)^2}} + \frac{r_s}{r_d} \frac{\left[\sqrt{1-(\theta_I/\theta_M)^2}\right]^3}{(\theta_I/\theta_M)} \right\} + \mathcal{O}\big(\boldsymbol{\delta}^3\big). \tag{12}$$

The embedded lens equation was then obtained by eliminating $\tilde{\phi}_1$ from Eqs. (6) and (7) of

[4] using Eq. (12),

$$
\begin{aligned}
\theta_S = \theta_I - \frac{\theta_E^2}{\theta_M} \Bigg[\!\!\Bigg[& \frac{\left[\sqrt{1-(\theta_I/\theta_M)^2}\right]^3}{(\theta_I/\theta_M)} + \boldsymbol{\delta}^2 \Bigg\{ \frac{r_s}{r_d} \Bigg[\frac{15}{16} \frac{\cos^{-1}(\theta_I/\theta_M)}{(\theta_I/\theta_M)^2} \\
& + \frac{1}{16} \frac{\sqrt{1-(\theta_I/\theta_M)^2}}{(\theta_I/\theta_M)} \left[3 - 14(\theta_I/\theta_M)^2 + 20(\theta_I/\theta_M)^4\right] - \frac{3}{4}(\theta_I/\theta_M) \log \frac{1+\sqrt{1-(\theta_I/\theta_M)^2}}{1-\sqrt{1-(\theta_I/\theta_M)^2}} \Bigg] \\
& - \frac{1}{2}\beta_d \theta_M \Bigg[(\theta_I/\theta_M)\sqrt{1-(\theta_I/\theta_M)^2} \Bigg(1 - (\theta_I/\theta_M)^2 - \frac{2}{3}\frac{\chi_d}{\chi_{ds}} \left[4 - (\theta_I/\theta_M)^2\right] \Bigg) \\
& + \frac{\chi_d}{\chi_{ds}} (\theta_I/\theta_M) \log \frac{1+\sqrt{1-(\theta_I/\theta_M)^2}}{1-\sqrt{1-(\theta_I/\theta_M)^2}} \Bigg] \\
& + \frac{1}{6}\theta_M^2 \Bigg[(\theta_I/\theta_M)\sqrt{1-(\theta_I/\theta_M)^2} \Bigg(\left[1 + 2(\theta_I/\theta_M)^2\right] + 3\frac{\chi_d}{\chi_{ds}} \left[1 - (\theta_I/\theta_M)^2\right] \Bigg) \Bigg] \Bigg\} + \mathcal{O}\big(\boldsymbol{\delta}^3\big) \Bigg]\!\!\Bigg].
\end{aligned}
\tag{13}
$$

The simplified lens equation (5) is obtained by dropping all correction terms of order $\boldsymbol{\delta}^2$ and higher in Eq. (13). To the order of accuracy needed to obtain Eq. (4) it is sufficient to replace the angle $\tilde{\phi}_1$ used in [4] by θ_I using only terms up to order $\boldsymbol{\delta}^1$ of Eq. (12). The geometrical part of the time delay given in Eq. (4) was obtained by using Eq. (10) of [2] combined with Eq. (7) of [4]. The potential part of the time delay given in Eq. (4) was obtained by eliminating $\tilde{\phi}_1$ in Eq. (23) of [4]. The simplified embedded lens equation (5) is then re-affirmed, as expected, by applying Fermat's least time principle to Eq. (4). Knowing Eq. (5) is sufficient to reproduce the image properties for the embedded point mass accurate to order $\boldsymbol{\delta}^1$.

The absence of terms of order $\boldsymbol{\delta}^1$ in Eqs. (13) and (4) was surprising since they were previously present when other impact variables were used. When the lens equation and the time delay were previously given in [1–4] as functions of r_0 and/or $\tilde{\phi}_1$, β_d terms (terms of order $\boldsymbol{\delta}^1$) were actually present just as they were in the bending angle α. What we see in Eqs. (4)-(10) is that when θ_I is used as the independent variable, terms of order $\boldsymbol{\delta}^1$ all vanish, including β_d terms, and hence Λ is no longer present at this order. We find this somewhat surprising in light of an earlier controversy [19–22], settled in the affirmative, about the existence of an effect on the bending angle α by the cosmological constant. However, we do find that when terms of order $\boldsymbol{\delta}^2$ are kept in the lens equation (parameterized by θ_I), Λ is once again explicitly present [23, 24], see Eq. (13).

The point mass theory is of limited usefulness on the scale of clusters. Fortunately the above is easily generalized to lenses with arbitrarily distributed mass, once it is observed that the order $\boldsymbol{\delta}^1$ lens equation (5) is the same as the classical lens equation for the sum of a point mass and a distributed mass lens with negative projected surface mass density

$$\Sigma(\theta_I) = \Sigma_{\rm cr}\kappa = \frac{c^2 D_s}{4\pi G D_d D_{ds}}\kappa. \tag{14}$$

Here κ is from Eq. (9) and $\Sigma_{\rm cr}$ is the conventional critical surface mass density [17]. This leads to the immediate observation that we can generalize, to this order of accuracy, lens equation (5) to include any transparent spherically symmetric mass

$$\theta_S = \theta_I - \frac{\theta_E^2}{\theta_I}\left[f(\theta_I) - \left(1 - \left[\sqrt{1-(\theta_I/\theta_M)^2}\right]^3\right)\right], \tag{15}$$

where $f(\theta_I)$ is the fraction of the actual distributed mass lens within the impact cylinder defined by θ_I. Because an exact Einstein model is known, the Lemaitre-Tolman-Bondi metrics [25–27] embedded in FLRW, this result can be confirmed by rigorously extending the work done in [1–4]. The generalization to any distributed lens, not necessarily spherically symmetric, is also obvious

$$\boldsymbol{\theta}_S = \boldsymbol{\theta}_I + \frac{D_{ds}}{D_s}\boldsymbol{\alpha}_0(\boldsymbol{\theta}_I) + \boldsymbol{\theta}_I\left(\frac{\theta_E}{|\boldsymbol{\theta}_I|}\right)^2\left(1 - \left[\sqrt{1-(|\boldsymbol{\theta}_I|/\theta_M)^2}\right]^3\right), \tag{16}$$

where $\boldsymbol{\alpha}_0$ is the conventional bending angle without embedding. This result cannot be readily confirmed because the relevant Einstein solution is not known. Nonetheless, it should be correct to order $\boldsymbol{\delta}^1$. Image properties for these transparent lenses can be obtained much as they were for the point mass in Eqs. (6)-(10). Because of the simple dependence of these lowest order embedded lens equations on angular size distances, they should also be valid for any FLRW background models, not just flat cosmologies. To extend the higher order lens equation (13) to non-flat backgrounds will require additional work.

Acknowledgments: NSF AST-0707704, and US DOE Grant DE-FG02-07ER41517 and Support for Program number HST-GO-12298.05-A was provided by NASA through a grant from the Space Telescope Science Institute, which is operated by the Association of Universities for Research in Astronomy, Incorporated, under NASA contract NAS5-26555.

---

[1] R. Kantowski, B. Chen, and X. Dai, Astrophys. J. **718**, 913 (2010).

[2] B. Chen, R. Kantowski, and X. Dai, Phys. Rev. D**82**, 043005 (2010).

[3] B. Chen, R. Kantowski, and X. Dai, Phys. Rev. D**84**, 083004 (2011).

[4] R. Kantowski, B. Chen, and X. Dai, Phys. Rev. D**86**, 043009 (2012).

[5] P. Schneider and A. Weiss, Astronomy & Astro **143**, 413 (1985).

[6] R. Blandford and R. Narayan, Astrophys. J. **310**, 568 (1986).

[7] A. Einstein and E. G. Straus, Rev. Mod. Phys. **17**, 120 (1945).

[8] E. Schücking, Z. Phys. **137**, 595 (1954).

[9] F. Kottler, Ann. Phys. (Leipzig) **361**, 401 (1918).

[10] R. Kantowski, Astrophys. J. 155, **89** (1969).

[11] C. C. Dyer and R. C. Roeder, Astrophys. J. **189**, 167 (1974).

[12] P. Schneider and A. Weis, Astrophys. J., **327**, 526 (1988).

[13] R. Kantowski, T. Vaughan, and D. Branch Astrophys. J. **447**, 35 (1995).

[14] E. W. Kolb, V. Marra, and S. Matarrese, Gen. Relativ. Gravit. **42**, 1399 (2010).

[15] C. Clarkson, G. F. R. Ellis, A. Faltenbacher, R. Maartens, O. Umeh, and J-P Uzan, Mon. Not. R. Astron. Soc. **426**, 1121 (2012).

[16] M. J. Rees and D. W. Sciama, Nature **217**, 511 (1968).

[17] P. Schneider, J Ehlers, and E. E. Falco, *Gravitational Lenses* (Springer-Verlag, Berlin, 1992).

[18] J. H. Cooke and R. Kantowski, Ap. J. **195**, L11 (1975).

[19] W. Rindler and M. Ishak, Phys. Rev. D**76**, 043006 (2007).

[20] M. Sereno, Phys. Rev. Lett.**102**, 021301 (2009).

[21] T. Schücker, Gen. Relativ. Gravit. **41**, 67 (2009).

[22] M. Ishak, W. Rindler, and J. Dossett, Mon. Not. R. Astron. Soc. **403**, 21521 (2010).

[23] T. Schücker, Gen. Relativ. Gravit. **42**, 1991 (2010).

[24] K.-E. Boudjemaa, M. Guenouche, and S. R. Zouzou, Gen. Relativ. Gravit. **43**, 1707 (2011).

[25] G. Lemaitre, Ann. Soc. Bruxelles **A53**, 51 (1933).

[26] R. C. Tolman, Proc. Natl. Acad. Sci. **20**, 169 (1934).

[27] H. Bondi, Mon. Not. R. Astron. Soc. **107**, 410 (1947).